NOVEL CONTROL STRATEGY FOR GRID-CONNECTED PHOTOVOLTAIC ARRAYS

REZA NOROOZIAN[*1] AND GOVERG B. GHAREHPETIAN[2]

[1]*Department of Electrical Engineering, Faculty of Engineering, University of Zanjan, P.O. Box 45371-38791, Zanjan, Iran.*
[2]*Faculty of Electrical Engineering, Amirkabir University of Technology, Tehran, Iran.*

[*]*corresponding author: noroozian@znu.ac.ir*

ABSTRACT: PV generation systems have received much attention in recent years due to their suitable properties which offer important economic benefits. However, they are developing increasingly fast as a renewable energy resource. In this work, the configuration of PV generation systems, a dynamic model for PV modules, and their power electronic interfacing have been presented. A novel control strategy for the DC-DC converter has been developed in order to extract the maximum amount of power from the PV array. Also, a novel control strategy, which is based on a $d - q$ rotating reference frame, has been proposed for the DC-AC converter. The proposed controllers have been used to transfer the PV output power and synchronize the interfacing power converters with the AC grid. The controller designs for different operating conditions of DC-AC converter, using the average large signal model, have been presented. Based on the dynamic models, a simulation model for the PV generation systems has been developed using PSCAD/EMTDC. Simulation studies have been carried out to verify the dynamic performance of grid-connected PV systems under different operating conditions. The simulation results show that the novel control structure can transfer DC energy from the PV array, compensate the power factor of the AC grid, and improve the dynamic behavior of the grid-connected PV system. The simulation results show the effectiveness of the suggested control systems in grid-connected mode.

ABSTRAK: Sistem penjanaan PV mendapat perhatian di dalam tahun kebelakangan ini kerana sifatnya yang sesuai dan ia menawarkan faedah ekonomi yang penting. Ia semakin pesat berkembang sebagai sumber tenaga yang boleh diperbaharui. Kajian ini membentangkan konfigurasi bagi sistem penjanaan PV, model dinamik untuk modul PV dan pengantaramukaan elektronik kuasa. Satu strategi kawalan baru untuk Penukar DC-DC telah dibina untuk mengekstrak jumlah kuasa maksima daripada pelbagai PV. Juga, strategi kawalan baru yang berdasarkan kepada rangka rujukan berputar $d - q$, telah dicadangkan untuk penukar DC-AC. Alat kawalan yang dicadangkan telah digunakan untuk memindahkan kuasa output PV dan menyegerakkan pengantaramukaan penukar dengan grid AC. Reka bentuk alat kawalan untuk keadaan operasi Penukar DC-AC yang berbeza telah dibentangkan dengan menggunakan purata model signal besar. Berdasarkan model dinamik, model simulasi bagi sistem penjanaan PV telah dibina dengan menggunakan perisian PSCAD/EMTDC. Kajian simulasi telah dijalankan untuk mengesahkan prestasi dinamik sistem PV tersambung grid di dalam keadaan operasi yang berbeza. Keputusan simulasi menunjukkan bahawa struktur kawalan baru boleh memindahkan tenaga DC dari tatasusunan PV, mengimbangi faktor kuasa AC grid dan memperbaiki tingkah laku dinamik sistem PV tersambung grid. Keputusan simulasi menunjukkan keberkesanan sistem kawalan yang dicadangkan dalam mod tersambung grid.

1. INTRODUCTION

Solar energy has great potential to supply energy for the future with minimum impact on the environment since solar energy is clean, pollution-free, and inexhaustible. With the decrease in the price of Photovoltaic (PV) modules and the increase in the price of conventional petrochemical fuels for energy generation, the application of the PV generation system becomes more practical, feasible, and realizable [1, 2].

PV cells are normally connected together to make up modules, which can be combined into PV arrays as required. Therefore, power electronic circuits are an enabling technology that is necessary to convert Direct Current (DC) electrical power generated by a PV array into usable Alternating Current (AC) power for grid support or supplying special loads [1-5].

The PV array is interfaced with the utility network via boost DC-DC converters and a three-phase Pulse-Width Modulation (PWM) DC-AC converter. The DC voltage generated by a PV array varies widely but is generally low in magnitude. Therefore, a boost DC-DC converter is necessary to generate a regulated higher DC voltage for desired converter input voltage. Generally, the grid connected PV systems extract maximum power from the PV arrays. The Maximum Power Point Tracking (MPPT) technique is usually associated with DC–DC converters. The DC-AC Voltage Source Converter (VSC) is employed to interface PV array energy systems with the utility grid under both on-grid and off-grid operations [1, 3]. The DC–AC converter injects sinusoidal current into the grid, controlling the power factor [1-5]. Many different topologies of power inverter for grid connected PV systems have been used. The parallel inverter with a common DC bus has optimal operation strategy [6]. In this topology, the power inverter converts the DC output of the PV modules into an AC output.

The control strategy of the DC-AC converter should be able to deliver a preset amount of active and reactive power to the grid or supply an isolated unbalanced AC load by balanced AC voltage with constant magnitude and frequency. Therefore, the DC-AC converter controller in on-grid mode controls the active and reactive power flows to the utility grid. In [7-11], a novel and simple control system based on instantaneous power control strategy has been developed for DC-AC converters.

This paper presents a dynamic model of a PV array and its power electronic interfacing. A novel control strategy of the DC-DC converter has been developed, too, in order to extract the maximum amount of power from the PV array. Also, a new control strategy based on a $d - q$ rotating reference frame has been presented for the DC-AC converter.

This system is capable of transferring energy from the PV power plant to a three-phase AC system with control of active and reactive power and without injecting harmonic currents. Reactive power compensation at the Point of Common Coupling (PCC) is investigated, too. Also, the injected reactive power can be dynamically controlled. The effectiveness of the proposed system has been verified by simulations. The simulation results show that the novel control structure can adjust the DC energy, compensate for the power factor of the utility grid and improve the dynamic behavior of the grid-connected PV system. This paper is organized as follows: the grid-connected PV system configuration is described in Section 2. In Section 3, the dynamic models for the PV module are introduced. The proposed power control converters are presented Section 4. Sections 5 and 6 discuss the simulation results and conclusion, respectively.

2. GRID-CONNECTED PV SYSTEM CONFIGURATION

Figure 1 shows the block diagram of the grid-connected PV generation system analyzed in this paper. A validated 200 W PV module is used to model the PV power plant [12]. The PV power plant consists of five PV modules connected in parallel. The DC-DC boost converters drain the energy from the photovoltaic module and feed the DC bus capacitor with MPPT control. The DC-DC converter is used to boost the low DC voltage. In this paper, the DC bus voltage (DC-DC converter output) is $V_{dc} = 750$ V. The proposed control structure for each DC-DC converter is designed to keep this DC bus voltage within a specified limit (i.e., ±5%). The DC-AC converter is a three-phase six-switch VSC current controlled with neutral clamped DC capacitors, that interfaces the DC bus with a utility 220 V / 240 VAC grid. An LC filter has been used at the output of the converter to filter the switching frequency harmonics. The DC-AC converter controller controls the active and reactive power delivered from the PV generation system to the utility grid. Supercapacitors or battery banks are connected to the DC bus to provide energy storage capability under different operating conditions.
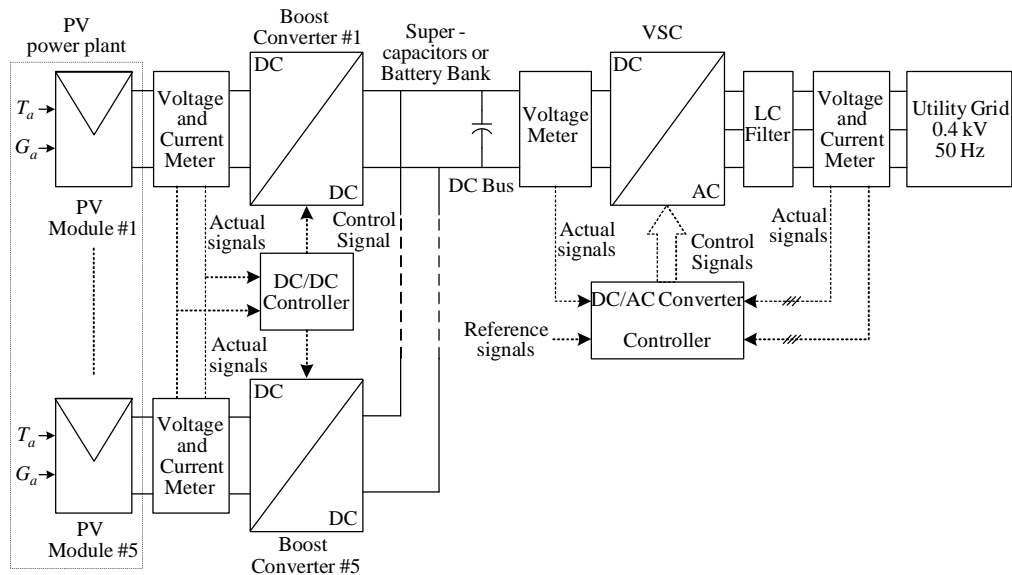

Fig. 1: Block diagram of the grid-connected PV generation system.

3. DYNAMIC MODELS FOR THE PV MODULE

In an array, several PV modules have been connected in a series and parallel to obtain a suitable power rating. Also, the PV cells are connected in series and parallel in a module. The most commonly used model for a PV cell is the DC current source (I_L) with a diode connected in parallel as shown in Fig. 2 [13, 14]. The DC source current depends on ambient temperature (T_a) and solar irradiation (G_a). The resistance R_s represents the losses and voltage drop in the circuit. Also, the resistance R_p represents the reverse of the diode. In this paper, the PV dynamic model, reported in [15], has been used to model the PV arrays. The PV array can be modeled by temperature and irradiation dependent $V - I$ characteristic. It is important to use the PV system near its maximum power point to increase the efficiency of the photovoltaic array. Therefore, the optimal operating voltage has to be applied to achieve maximum power. This can be realized using a MPPT algorithm [4, 5]. In this study, a suitable voltage-based MPPT controller for the optimum

operation of the PV modules has been used. The parameters of a 200-W PV data (SPR-200-BLK [12]) have been used for PV array simulations. The output characteristics curves for the PV array subjected to varying solar irradiance are shown Fig. 3. As can be seen in Fig. 3, variations of solar irradiance have a great impact on the PV array's generated power [16-18].
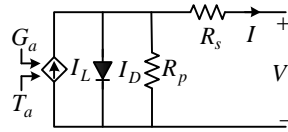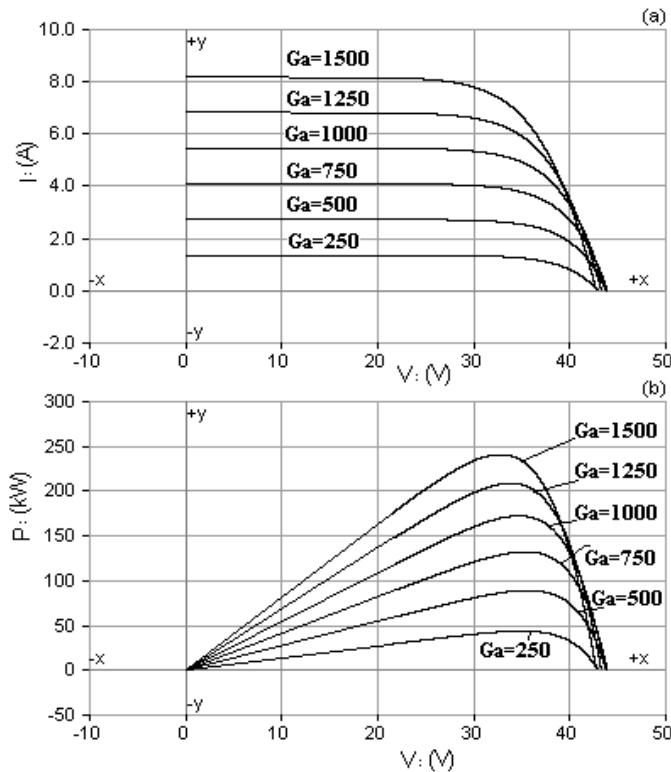
Fig. 2: Model of a single PV cell.

Fig. 3: Characteristic curves of the PV array with different solar irradiations.

4. PROPOSED CONTROL OF POWER CONVERTERS

The current controller for the power converter can be a closed loop PWM scheme, such as Hysteresis Current Control (HCC), linear PWM, predictive controllers, optimized controllers, neural networks, and fuzzy logic controller systems [7-11]. In comparison to open loop PWM techniques, closed loop PWM schemes have several considerable advantages, such as extremely good dynamics, instantaneous peak current control, and prevention of overload and pulse dropping problems [7-11]. HCC has stability, which is provided by maintaining the current errors within the hysteresis band. Thus, HCC has been selected in this paper. The power converters' controller provides the reference current for the HCC. Its instantaneous power regulation has a much faster response when compared to average power regulation [16]. Therefore, instantaneous power regulation has been used for the converter in this paper. As a result, the reference currents for the closed loop PWM

scheme of the converter are calculated using the instantaneous active and reactive powers concept. The instantaneous powers can be expressed in either a synchronous or a stationary reference frame. In this paper, a synchronously rotating frame is used for the converter reference current generation.

4.1 Control System of Boost Converters

The proposed control strategy of the DC-DC boost converter is shown in Fig. 4. This system specifies the reference current, i_{fpv}^{ref} for the HCC scheme. The HCC system regulates the boost converter inductor current, i_{fpv}, within the hysteresis band. The converter manages the amount of the current injected to the DC bus.
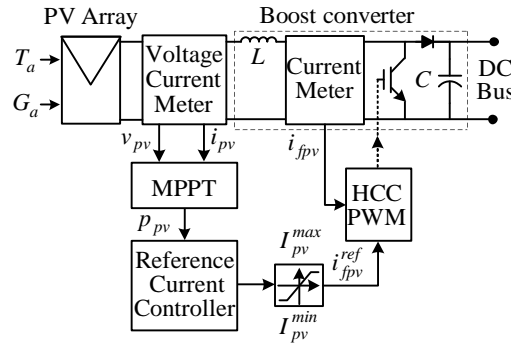

Fig. 4: Proposed control system for each boost converter.

In this control structure, the reference active power, p_{pv} is obtained by the MPPT control algorithm. The reference current, i_{fpv}^{ref}, is expressed as:

$$i_{fpv}^{ref} = \frac{p_{pv}}{v_{pv}} \tag{1}$$

The comparison of the calculated reference currents, i_{fpv}^{ref}, with the actual current generated by the boost converter, i_{fpv} will result in an error signal, which is fed to the HCC system in order to determine the switching pattern of the DC-DC boost converter.

The inductor of each boost converter is designed to make its current track the reference current within the hysteresis band. Thus, the inductor L for each boost converter is obtained by the following equation [7]:

$$L = \frac{4V_{dc}^{ref}}{h.f_{s,\max}} \tag{2}$$

where, h is the hysteresis band and $f_{s,max}$ is the maximum switching frequency of the boost converter.

4.2 Control Structure of the DC-AC Converter

The DC-AC voltage source converter must act as a power controller between the utility grid and the DC bus. The grid-connected (or on-grid) operation allows the converter to operate parallel to the grid, providing grid support. The average large signal model of the DC-AC converter is shown in Fig. 5. This converter has been modeled with three

current sources i_{fa}^{ref}, i_{fb}^{ref} and i_{fc}^{ref}. The converter manages the current injected into the utility. Since the current generated from the converter can be controlled independently from the AC voltage, the active and reactive power controls are decoupled. As can be seen in Fig. 5, the input signals of the DC-AC converter are source phase voltages, (v_{sa}, v_{sb}, and v_{sc}), the source phase currents, (i_{sa}, i_{sb} and i_{sc}), three-phase output currents for this converter (i_{fa}, i_{fb} and i_{fc}), the DC bus voltage (v_{dc}), the reference of the DC bus voltage (V_{dc}^{ref}), and the output active power of the PV power plant (P_{pvs}). L_f is the inductance of the converter filter. R_g and L_g are the resistance and inductance of the AC grid, respectively. This controller uses the HCC switching technique. As can be seen in Fig. 5, we have:

$$\begin{bmatrix} i_{sa} \\ i_{sb} \\ i_{sc} \end{bmatrix} = -\begin{bmatrix} i_{fa} \\ i_{fb} \\ i_{fc} \end{bmatrix} \tag{3}$$
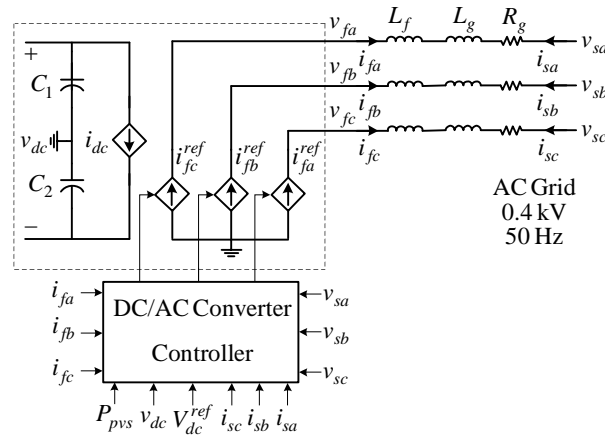

Fig. 5: Average large signal model of the DC-AC converter.

Figure 6 shows the DC-AC converter control system in the grid-connected operation. In this paper, a novel control strategy has been designed based on the instantaneous power control strategy. Using $d - q$ reference frames, the coupled dynamics of the current tracking problem have been transformed into decoupled dynamics. Applying the Park transformation, the source currents and voltages are converted from the three-phase coordinates to a synchronously rotating frame by Eqs. (4) and (5), where θ is the instantaneous angle of the network voltage vector, which is obtained from the Phase Locked Loop (PLL) circuit.

$$\begin{bmatrix} v_{sd} \\ v_{sq} \end{bmatrix} = T_{dq} \begin{bmatrix} v_{sa} \\ v_{sb} \\ v_{sc} \end{bmatrix} \tag{4}$$

$$\begin{bmatrix} i_{sd} \\ i_{sq} \end{bmatrix} = T_{dq} \begin{bmatrix} i_{sa} \\ i_{sb} \\ i_{sc} \end{bmatrix} \tag{5}$$

$$T_{dq} = \frac{2}{3}\begin{bmatrix} \cos(\omega t) & \cos(\omega t - 120^\circ) & \cos(\omega t + 120^\circ) \\ -\sin(\omega t) & -\sin(\omega t - 120^\circ) & -\sin(\omega t + 120^\circ) \end{bmatrix}$$

In these equations, v_{sd} and v_{sq} are the $d - q$ components of the source voltages, in the synchronously rotating frame, respectively. i_{sd} and i_{sq} are the $d - q$ components of the source currents. The instantaneous active power is given as follows:

$$p = \bar{p} + \tilde{p} = v_{sd}i_{sd} + v_{sq}i_{sq} \tag{6}$$

The superscripts (-) and (~) in Eq. (6) denote the average and oscillatory components of the instantaneous active power, respectively. $\bar{p}$ is the average value of the instantaneous active power (p). This is the energy per time unit transferred from the source to the load, in a balanced way through 3 phases. $\tilde{p}$ is the oscillating term of the instantaneous active power. It is the energy per time unit, which is exchanged between the power source and the load, through 3 phases. In this paper, the instantaneous active power components, which will be injected by the DC-AC converter to the AC grid, (p_{ref}), include the undesired power quality problems (harmonics, unbalance and reactive power) and the energy available in the PV generating system, i.e.:

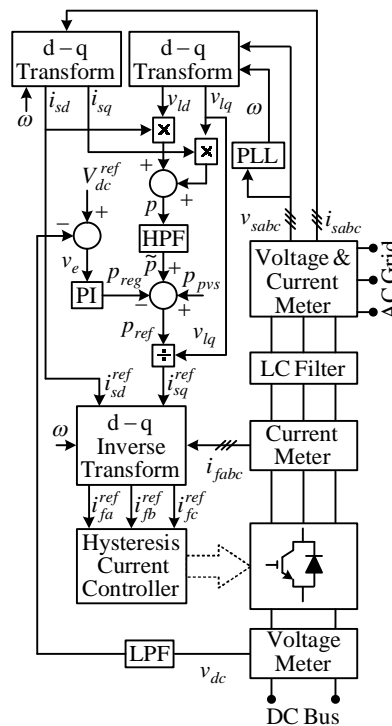$$p_{ref} = p_{pvs} - p_{reg} + \tilde{p} \tag{7}$$

Fig. 6: Control System of the DC-AC converter.

In Fig. 6, the power obtained by the MPPT controller, p_{pvs} corresponds to the output power available from the PV arrays. The instantaneous active power is passed through the High Pass Filter (HPF), which removes the low frequency components of the active power. This filtered signal is used for the DC-AC converter, which compensates the harmonics and unbalancing.

The DC bus voltage regulator determines the power p_{reg}. The DC bus voltage passes through a PI controller and then it is subtracted from p_{pvs}. This power balance and switching losses can decrease the DC bus capacitor. Let the voltage error, v_e between the reference DC bus voltage and the measured DC capacitors voltages be defined as follows:

$$v_e = V_{dc,ref} - v_{dc} \tag{8}$$

Adjusting the gains of the PI compensators, a fast tracking and zero steady state errors can be achieved. The voltage error has been regulated by a proportional-integral (PI) controller, then, we have:

$$p_{reg} = K_P v_e + K_I \int v_e \, dt \tag{9}$$

The transformation of the balanced source voltages $d – q$ axis of the synchronously rotating frame results in the following equation:

$$v_{sd} = 0 \text{ and } v_{sq} = 0.4\sqrt{\frac{2}{3}} \tag{10}$$

Substituting the Eq. (6) into Eq. (10) yields:

$$i_{sq} = \frac{p}{v_{sq}} \tag{11}$$

Using Eq. (11), the reference current of the DC-AC converter in q axis can be expressed by the following equation:

$$i_{sq}^{ref} = \frac{p_{ref}}{v_q} \tag{12}$$

where, i_{sq}^{ref} is the direct component of the reference current of the converter. This component is also responsible for feeding the losses in both the converter and the capacitor.

The resultant d component is responsible for the reactive power flow through the utility network. To compensate for the reactive component, the quadrature component of the reference current of the DC-AC converter can be equal to the quadrature component of the source current:

$$i_{sd}^{ref} = i_{sd} \tag{13}$$

Considering the reactive power generation limit of the PV plant and the size of DC-AC converter, a limiter can be used for i_{sd}^{ref} to represent the permissible range. The $d – q$ inverse transformation block, shown in Fig. 6, calculates the three-phase current references to be fed into the HCC scheme. Thus:

$$\begin{bmatrix} i_{sa}^{ref} \\ i_{sb}^{ref} \\ i_{sc}^{ref} \end{bmatrix} = T_{abc} \begin{bmatrix} i_{sd}^{ref} \\ i_{sq}^{ref} \end{bmatrix} \tag{14}$$

$$T_{abc} = \begin{bmatrix} \cos(\omega t) & -\sin(\omega t) \\ \cos(\omega t - 120^\circ) & -\sin(\omega t - 120^\circ) \\ \cos(\omega t + 120^\circ) & -\sin(\omega t + 120^\circ) \end{bmatrix}$$

$$\begin{bmatrix} i_{fa}^{ref} \\ i_{fb}^{ref} \\ i_{fc}^{ref} \end{bmatrix} = - \begin{bmatrix} i_{sa}^{ref} \\ i_{sb}^{ref} \\ i_{sc}^{ref} \end{bmatrix} \tag{15}$$

HCC is a closed loop control for the current of DC-AC converter. The comparison of the calculated reference currents and the actual compensator currents generated by the DC-AC converter will result in an error signal, which controls the switches of the converter. When the error reaches the upper limit of the hysteresis comparator, IGBTs are switched to increase the current, and when the error reaches the lower limit, the current is forced to decrease. This procedure leads to the fast dynamic response that characterizes HCC among other current control techniques. The range of the error signal, h, directly controls the amount of ripples in the output current of the DC-AC converter and is called the hysteresis band. The current is forced to stay within these limits even while the reference current is changing.

5. SIMULATION RESULTS

In this paper, to evaluate the performance of the PV generation system, the proposed control structure and the on-grid operating condition have been modeled and simulated by PSACD/EMTDC. The simulation results show the ability of the proposed system to transfer DC energy from the PV unit to the AC grid with high power quality under on-grid operating conditions. The novel control strategy of the DC-AC converter with neutral clamped DC capacitors has been studied in on-grid operation modes. In the simulations, the rated power for each PV unit is assumed to be 25 kW. The ambient temperature (T_a) is assumed to be 25 ºC. It is also assumed that the reference DC voltage is 750 V and the nominal droop is 5 percent.

5.1 Solar Radiation Changes

In this section, the evolution of some characteristics of the grid-connected PV system during daytime and nighttime modes in solar radiation has been studied. The solar irradiance, G_a is shown in Fig. 7(a). As shown in Fig. 7(a), the irradiance has been changed from $0.8\cos(2\pi t)$ kW/m^2 to zero at t = 2.25 s and then from zero to $0.8\cos(2\pi t)$ kW/m^2 at t = 2.75 s. When $1.75 < t < 2.25$ s and $2.75 < t < 3.25$ s, the all PV units are operated in daytime mode. When $1.50 < t < 1.75$ s, $1.25 < t < 1.75$ s and $3.25 < t < 3.50$ s, all PV units are operated in nighttime mode.

Figure 7(b) shows the instantaneous active power, P, and the power of the PV plant (P_{pvz}). As can be seen in Fig. 7(b), the active power injected into the AC grid has changed nighttime and daytime operating conditions. It is obvious that the PV generation system delivers active power to the grid that matches the solar irradiance variations. It is also clear that the system can control the power injected into the grid and the system has an excellent dynamic performance. Also, the suggested control strategy for the DC-AC converters provides a reasonable response.
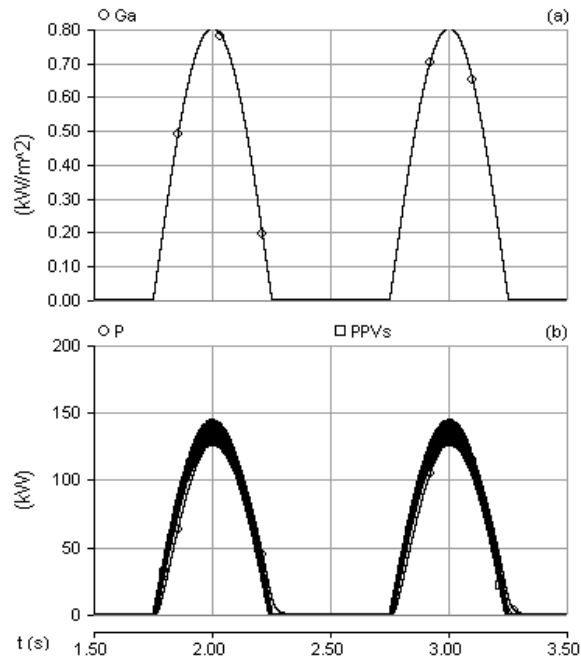
Fig. 7: (a) solar irradiance, and
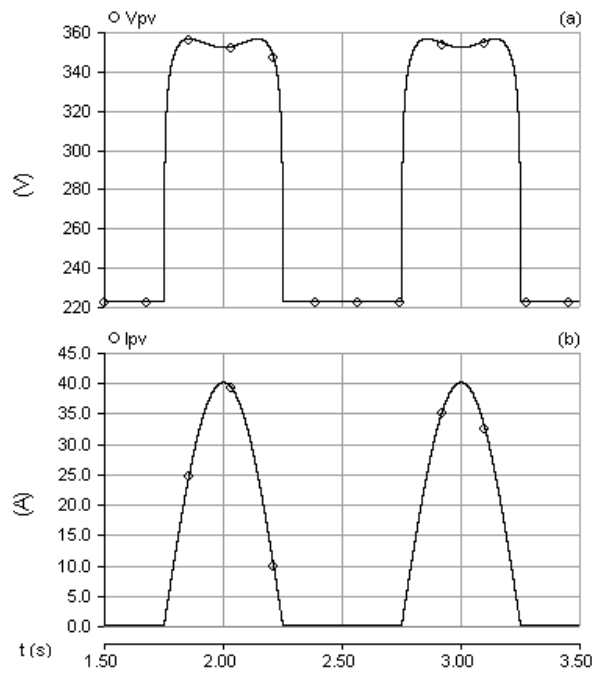(b) active power delivered to grid and power of PV plant.

Fig. 8: Output voltage and current of each PV module.

Figure 8 depicts the output voltage and current of each PV module. As shown in Fig. 8, the PV module current is severely affected by the solar radiance variation. However, the MPPT controller is operating well since the required results for the PV generating system have been obtained.

Figure 9 depicts the active power injected into the DC bus and the voltage of the DC bus (v_{dc}). Figure 9(a) depicts the active power injected into the DC bus. As shown in Fig. 9(a), the active power injected into the DC bus, using the PV power plant, increases and reaches to its reference value, which matches the above mentioned solar radiation changes. According to Fig. 9(b), the voltage of the DC bus experiences a swell while the PV power generated has been increased and returns to the nominal DC voltage. It is also clear that when the PV power generated has been decreased, the DC bus voltage experiences a sag phenomena. As can be seen, the DC bus voltages (v_{dc}) follow the DC voltage ($V_{dc,ref}$), which match together. Therefore, the real power extracted from the PV power plant can pass through the grid. It is also clear that when the PV power generated has been decreased, the DC network voltage experiences a sag phenomena.
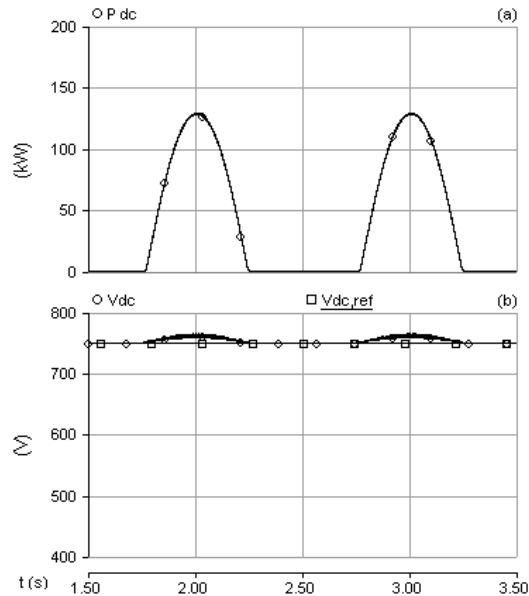

Fig. 9: (a) Output power from the DC bus and (b) DC bus voltage.

Figure 10 shows the grid-side phase voltage and the line current of the DC-AC converter. The three-phase voltages and currents are shown only for phase *a*. Similar wave-forms can be plotted for phases *b* and *c*. The line current changes with power reference variations, which flows into the utility grid. Therefore, the converter can deliver the PV generation system power to the grid with a low harmonic current. This verifies the effectiveness of the proposed control system. As can be seen in this figure, there is no phase leading-lagging between the grid-side line current and the voltage. They are in phase and sinusoidal. As a result, the proposed control system is capable of controlling the current injected into the grid at unity power factor by changing the DC-AC converter injected reactive power dynamically.

5.2 Voltage Dip in the AC Grid

In this section, the effect of the grid fault on the operation of the PV system has been studied. A three-phase fault at the AC grid has been simulated to model a voltage dip during the time period of t = 3.0 s till t = 3.1 s. Figure 11(a) and 11(b) indicate the phase to neutral voltage and the line current for three phases. According to Fig. 11(c), the phase to neutral voltage and line current (phase *a*) is in phase. This verifies the effectiveness of the novel control strategy for the DC-AC converter.
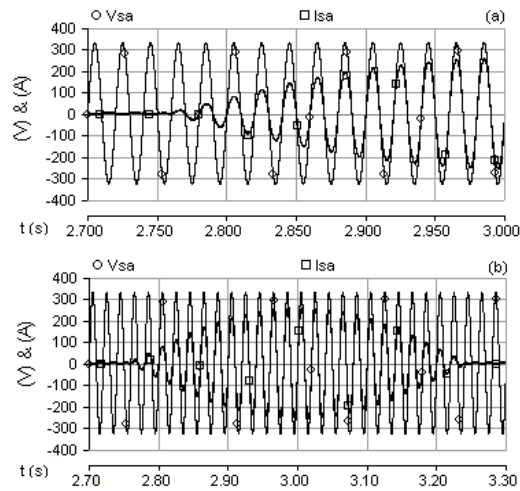
Fig. 10: Grid voltage and injected current for a step change from 1000 to 300 W/m^2 and from 300 to 800 W/m^2.
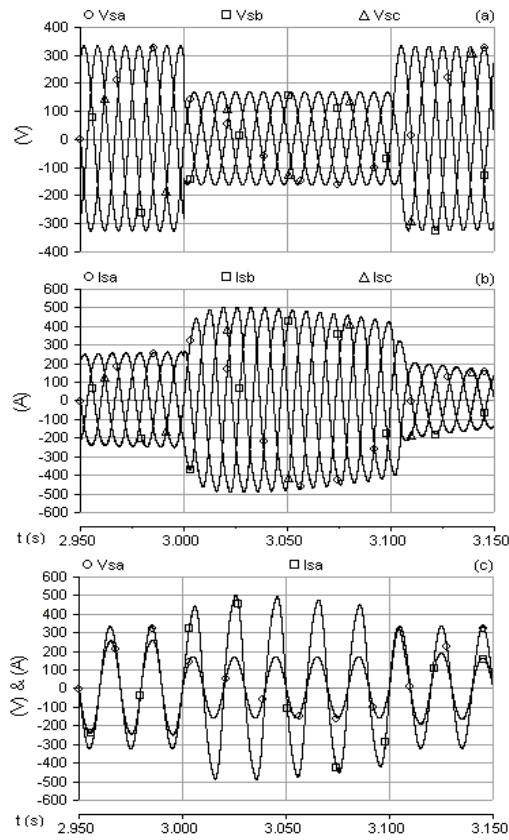

Fig.11: (a) Grid three phase voltage, (b) grid injected currents and (c) grid voltage and injected current.
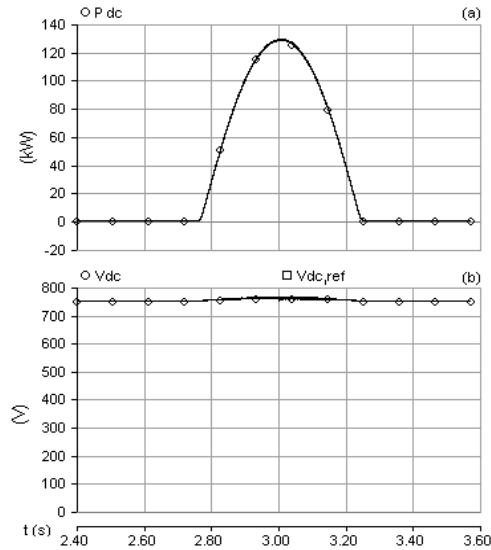
Fig. 12: (a) Output power from the DC bus and (b) DC bus voltage.

Figure 12(a) shows the active power injected into the DC bus. Considering Fig. 12(a), the voltage dip does not have an influence on the maximal power provided by the DC-DC converter. This is due to the DC bus capacitor, which acts as a buffer. Figure 12(b) shows the regulation of the DC bus voltage, which matches the grid connected conditions and is constant (750 V). Thereby, the real power extracted from the PV power plant can pass through the grid.

5.3 Frequency Variation of the Grid Voltage

The aim of this section is to study the effect of the network frequency variation on the grid-connected operation condition. The frequency variation has been applied to AC grid at t = 2.8 s (50.2 Hz) and at t = 3.0 s (50 Hz), which means a frequency variation of 0.2 Hz in 0.2 s. Figure 13(a) and 13(b) show the phase to neutral voltage and the line current for three phases. According to Fig. 13(c), the phase to neutral voltage and the line current (phase *a*) is in phase. This figure verifies the effectiveness of the novel control strategy for the DC-AC converter.

Figure 14 depicts the MPPT performance of the DC-DC converter and the DC bus voltage controllers. Both figures are independent of the frequency variation.

6. CONCLUSION

This paper presents a new control structure for a PV generation array in on-grid operation mode. The dynamic model of the PV modules and its power electronic interfaces has been presented. Also, a novel control strategy for grid-connected DC-AC converters with power factor control has been suggested. The current and DC voltage controllers have been used to transfer the PV power and synchronize the output converters with the grid. The controller designs for different operating conditions of the DC-AC converter have been presented using the average large signal model. The novel control structure, which is based on instantaneous power control strategy, has been used to control
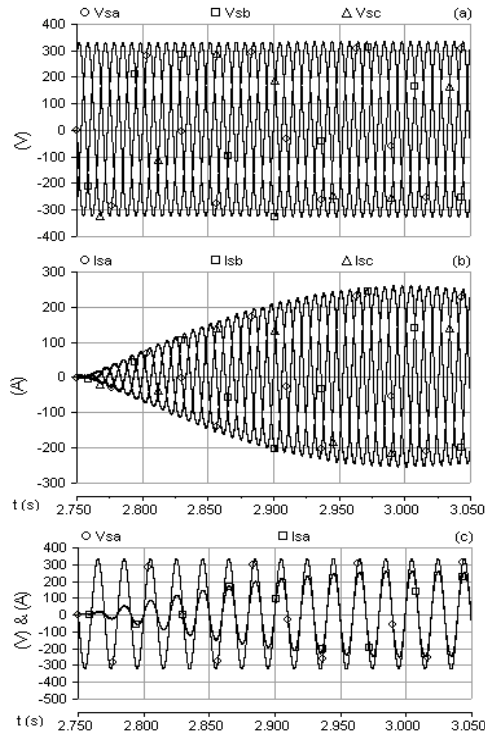
Fig. 13: Frequency variation effect on (a) grid three phase voltage,
(b) grid injected currents and (c) grid voltage and injected current.
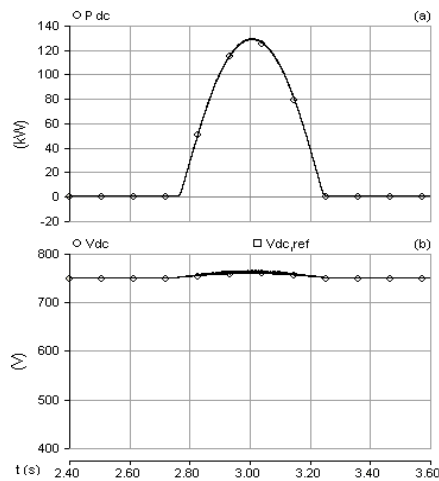
Fig. 14: Frequency variation effect on (a) Output power from the DC bus and
(b) DC bus voltage.

the active and reactive power delivered from the PV generation system to the utility grid. The simulation results based on PSCAD/EMTDC software demonstrate the effectiveness of the suggested control systems in grid-connected mode. Also, simulation results show that the proposed control strategies can control the power factor and regulate the reactive power for PV generating systems. In the simulations, the MPPT controller has been used to extract the optimal power from the PV array, while the DC bus voltage remains within acceptable limits.

REFERENCES

[1]   Hassaine L, Olias E, Quintero J, Haddadi M. (2009) Digital power factor control and reactive power regulation for grid-connected photovoltaic inverter. Renewable Energy, 34:315-321.

[2]   Hamrouni N, Jraidi M, Cherif A. (2008) New control strategy for 2-stage grid-connected photovoltaic power system. Renewable Energy, 33:2212-2221.

[3]   Barbosa PG, Rolim LGB, Watanabe EH, Hanitsch R. (1998) Control strategy for grid-connected DC-AC converters with load power factor correction. IEE Proceedings-Generation, Transmission and Distribution,145:487-492.

[4]   Koutroulis E, Kalaitzakis K, Voulgaris NC. (2001) Development of a microcontroller-based, photovoltaic maximum power point tracking control system. IEEE Tran. Power Electronics, 16:46-54.

[5]   Hua C, Shen C. (1998) Study of maximum power tracking techniques and control of DC-DC converters for photovoltaic power system. Proceedings of the 29th Annual IEEE Power Electronics Specialists, 1:86-93.

[6]   Hassaine L, OLias E, Quintero J, Salas V. (2014) Overview of power inverter topologies and control structures for grid connected photovoltaic systems. Renewable and Sustainable Energy Reviews, 30:796-807.

[7]   Noroozian R, Gharehpetian GB, Abedi M, Mahmoodi M. (2010) Grid-Tied and Stand-Alone operation of distributed generation modules aggregated by cascaded boost converters. J. Power Electronics, 10:97-105.

[8]   Mahmoodi M, Gharehpetian GB, Abedi M, Noroozian R. (2006) Novel and simple control strategy for fuel cell converters in DC distribution systems. Proceedings of IEEE PECon, 1:358-362.

[9]   Mahmoodi M, Gharehpetian GB, Abedi M, Noroozian R. (2006) A suitable control strategy for source converters and a novel load- generation voltage control scheme for DC voltage determination in DC distribution systems. Proceedings of IEEE PECon, 1:363-367.

[10] Mahmoodi M, Gharehpetian GB, Abedi M, Noroozian R. (2006) Control systems for independent operation of parallel dg units in DC distribution systems. Proceedings of IEEE PECon, 1:220-224.

[11] Noroozian R, Abedi M, Gharehpetian GB, Hosseini SH. (2010) Distributed resources and DC distribution system combination for high power quality. Int. J. Electrical Power and Energy Systems, 32:769-781.

[12] Sun Power Corporation [www.sunpowercorp.com]: Residential PV nodule SPR-200-BLK datasheet. Dec. 2004.

[13] Patel MR. (1999) Wind and solar power systems. CRC Press, U.S. Merchant Marine Academy, Kings Point, New York.

[14] Gow JA, Manning CD. (1999) Development of a photovoltaic array model for use in power electronic simulation studies. IEE Proceedings on Electric Power Applications, 146:193-200.

[15] Hansen AD, Sorensen P. (2000) Models for a Stand-Alone PV system. Riso National Laboratory: Roskilde, Denmark.

[16] Hassaine L, OLias E, Quintero J, Salas V. (2014) Overview of power inverter topologies and control structures for grid connected photovoltaic systems. Renewable and Sustainable Energy Reviews, 30:796–807.

[17] Molina MG, Espejo EJ. (2014) Modeling and simulation of grid-connected photovoltaic energy conversion systems. Int. J. Hydrogen Energy, 39:8702-8707.

[18] Ali SM, Pattanayak P, Sanki P, Sabat RR. (2012) Modeling and control of grid-connected hybrid photovoltaic distributed generation system. Int. J. Eng. Sci. Emerging Tech., 4:125-132.

ABBREVIATIONS

PWM	Pulse-Width modulation
PV	Photovoltaic
MPPT	Maximum Power Point Tracking
VSC	Voltage Source Converter
PCC	Point of Common Coupling
HCC	Hysteresis Current Control
PLL	Phase Locked Loop
HPF	High Pass Filter
LPF	Low Pass Filter
IGBT	Insulated Gate Bipolar Transistor